

---

**INVESTIGATIONS BY CAPACITANCE METHODS OF *n*-Si IRRADIATED BY ELECTRONS AT 450 °C****V.B.NEIMASH, M.M.KRAS'KO, A.M.KRAITCHINSKII, A.G. KOLOSYUK, V.V.VOITOVYCH, E.SIMOEN<sup>1</sup>, J.-M.RAFI<sup>1</sup>, C.CLAEYS<sup>1</sup>, J.VERSLUYS<sup>2</sup>, P.CLAUWS<sup>2</sup>**UDC 621.315.592  
© 2004**Institute of Physics, Nat. Acad. Sci. of Ukraine**  
(46, Nauky Prosp., Kyiv 03028, Ukraine),**IMEC**  
(Kapeldreef 75, B-3001 Leuven, Belgium),**Department of Solid-State Sciences, Gent University**  
(Krijgslaan 281 S1, B-9000 Gent, Belgium)

---

Using the methods of deep-level transmission spectroscopy (DLTS), the properties of radiation- and thermal-induced defects which are formed in silicon single crystals under an electron irradiation of 1 MeV at 450 °C have been investigated. Seven electron levels in the upper half and two levels in the lower half of the energy gap in Si have been revealed. Their energy and kinetics characteristics have been determined. It is found that secondary radiation-induced defects (RDs) are capable to migrate over large distances. An essential acceleration of the generation of oxygen thermal donors when exposed to the electron irradiation has been shown. The results obtained are interpreted by the radiation-enhanced diffusion of oxygen impurity atoms and the formation of various oxygen-vacancy complexes.

---

After four decades of investigations, the RDs in Si crystals do not lose scientific and technological interests [1, 2]. While the effects of irradiation were mainly studied earlier at low and ambient temperatures, the point of investigational attention shifted more recently towards the radiation-induced defect formation at elevated temperatures [3–7]. Beyond academic interest, it stems from the practical need in such radiation-induced defects which are stable at elevated temperatures. Their applications to the control over the electrical characteristics of Si and Si-based devices greatly enhance the efficiency of the radiation technologies, in particular, of those used in the production of power devices operating at temperatures above 100 °C. Of special interest are the effects of irradiation in the temperature interval 300–500 °C, where the intense formation of oxygen-

including thermal donors (OTDs) takes place. The application of the radiation-induced stimulation of the oxygen diffusion [8] to the OTD generation can provide new information about the mechanism of oxygen low-temperature diffusion enhancement in Si. The proper understanding of the mechanism is basically important in seeking the methods for the thermal stability enhancement of silicon-based devices.

Recently an original method of “hot” irradiation has been used to investigate the influence of the electron irradiation at 450 °C on the specific conductivity behavior of Czochralski-grown *n*-Si [8]. The peculiarity of this experimental technique consists in that the powerful beam of 1 MeV electrons is used to heat a specimen of silicon of several millimeters in width up to 450 °C. Due to thermal conductivity, the specimen is heated uniformly. But the capture of electrons and generation of electron-induced vacancies occurs in the surface layer of a width up to 1.5 mm. The application of surface methods for material investigation (e.g., the 4-probe method for conductivity measurement or capacitance methods) makes it possible to consider the irradiated (front) crystal surface as a specimen where radiation- and thermal-induced defects appear simultaneously, while the crystal surface not exposed to the electron beam (back) as a test specimen where only thermal defects are generated without radiation influence. In this case, the maximal identity is attained

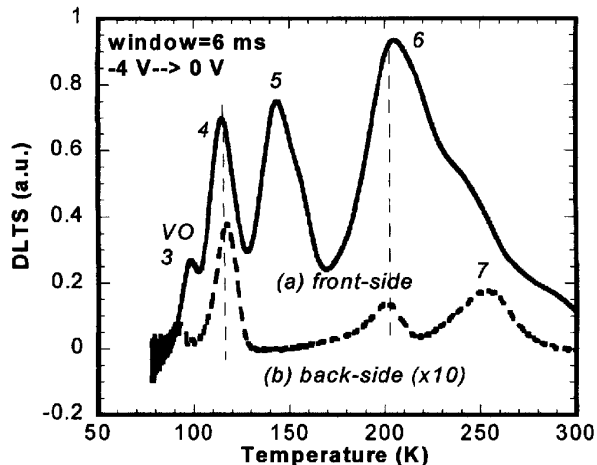


Fig. 1. DLTS spectra of the front and back sides of specimen 11-1 in the temperature interval 78–300 K. 1 MeV electron irradiation at 450 °C

for thermal regimes as well as for impurity and growth defect compositions. The results in [9] indicate that the electron irradiation is capable to enhance greatly the OTD generation and to create RDs of *p*-type. Afterwards, for specimens investigated in [9] by the 4-probe method, the method of DLTS was applied. Previous results for the temperature interval 78–300 K were published in [10]. It was shown that, at 450 °C, a wider RD spectrum is created in *n*-Si than that at ambient temperature. The aim of this work is to investigate the influence of the electron irradiation at 450 °C on the spectrum and numerical parameters of deep levels appearing in *n*-Si in more detail by using the DLTS method.

The “hot irradiation” procedure used in experiments was described in detail in [9, 10]. After the relevant chemical decontamination of the surfaces of the thermoradiated specimens 3 mm in thickness, Schottky barriers of gold 2 mm in diameter formed on their front and back sides. Eutectic alloys InGa and InHg were used for providing Ohmic junctions. Temperature dependences of the relaxation rate of the barrier capacity  $\Delta C/C$  were measured for specimens made up of various materials and after various durations of the thermoradiation treatment. The energy of deep level ionization was determined by the Arrhenius method. The free electron concentration was derived from the slope of the dependences  $1/C^2$  on the voltage  $U$  at a frequency of 1 MHz.

The initial specimen parameters are depicted in Table 1. Carbon impurity concentration is less than

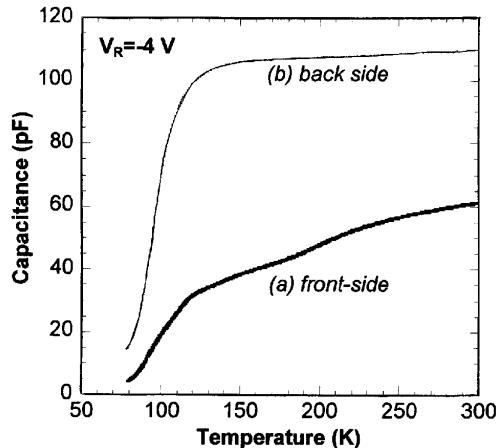


Fig. 2. Temperature dependences of the capacity for the front (a) and back (b) sides of specimen 11-1. 1 MeV electron irradiation at 450 °C

$5 \cdot 10^{16} \text{ cm}^{-1}$  for all specimens. In Table 1, the initial concentrations of the oxygen impurity and of free electrons before and after the treatment are denoted by  $N_{\text{O}}$ ,  $n_0$ , and  $n$ , respectively,  $t_{\text{TT}}$  is the duration of the thermoradiation treatment,  $\Phi_e$  is the exposure dose obtained during the thermoradiation treatment.

In Fig. 1, the DLTS spectra are shown for the front and back sides of the 11-1 specimen. Here, the spectrum for the back side is measured at the sensibility ten times as high as that for the front one. It is of interest that some peaks are observed on the back side which are also observed on the front side with much greater amplitudes. The absence of the Pool–Frenkel effect for all peaks observed proves their *p*-type. The fact that those levels are observed on the back side too, although in much less concentration than on the front one, means an essentially greater mobility of the RDs at 450 °C than that at ambient temperature. In contrast to estimations based on the data for electron radiation penetrability and the RD migration length at ambient temperature, the RDs are observed on the back side of the specimen as well. The peak amplitude ratios are different for front and back sides. The peak at 140 K on the back side is unobservable at all. This means the long-range migration of the secondary RDs with various speeds rather than

Table 1

| Specimen | $N_{\text{O}}, 10^{17} \text{ cm}^{-3}$ | $n_0, 10^{14} \text{ cm}^{-3}$ | $t_{\text{TT}}, \text{min}$ | $\Phi_e, 10^{16} \text{ cm}^{-2}$ | $n, 10^{14} \text{ cm}^{-3}$ |
|----------|---|--------------------------------|-----------------------------|-----------------------------------|------------------------------|
| 11-1     | 9                                       | 1.05                           | 120                         | 36                                | 2.55                         |
| 11-1     | 9                                       | 1.05                           | 120                         | 0                                 | 7.63                         |
| 3-1      | 2                                       | 4.7                            | 10                          | 3                                 | 3.7                          |
| 3-1      | 2                                       | 4.7                            | 10                          | 0                                 | 4.7                          |

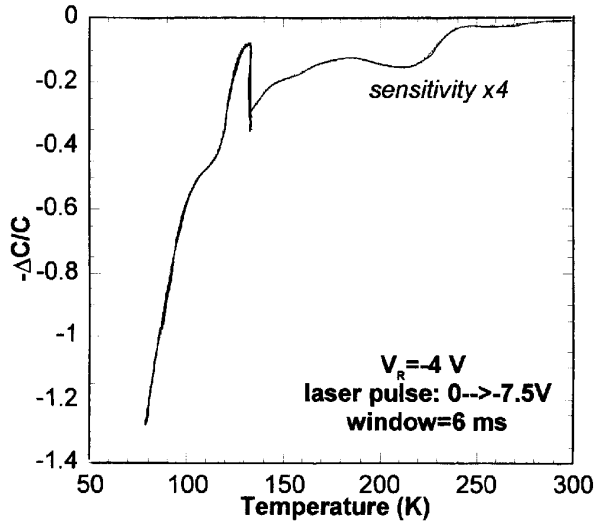


Fig. 3. Optically injected DLTS spectrum of the hole capture sites for the front side of specimen 11-1. 1 MeV electron irradiation

that of the primary RDs with a further creation of the secondary complexes.

One should be careful to the absolute values of the level ionization energy and the electron capture cross-section for these levels determined by the DLTS method using the specimens where the deep level concentration is comparable to that of minor impurities. The crystal under investigation belongs just to similar samples which is evidenced by the temperature dependence of the barrier capacity (see Fig. 2). One can see that the capacity diminishes to zero near 100 K where the shallowest level on the spectra in Fig. 1 inverts the charge. This means the approximate equality between the concentration of radiation acceptors and the sum of sulphur impurity and double OTD concentrations. It is interesting that the total “freezing-out” of the capacity takes place also on the crystal side oriented back to the electron beam, although here the RD concentration (according to Fig.1) is an order of magnitude less than that on the front side. It can be if the OTD concentration is also less to the same extent on the back side. This verifies the conclusion made in [9] that the irradiation greatly enhances the OTD generation. A discrepancy in numerical evaluations of the radiation effect obtained in [9] when analyzing the results of the 4-probe method (4–6 times) and the DLTS method (10 times) is probably a result of that the first estimation did not take into account the partial compensation of the conductivity

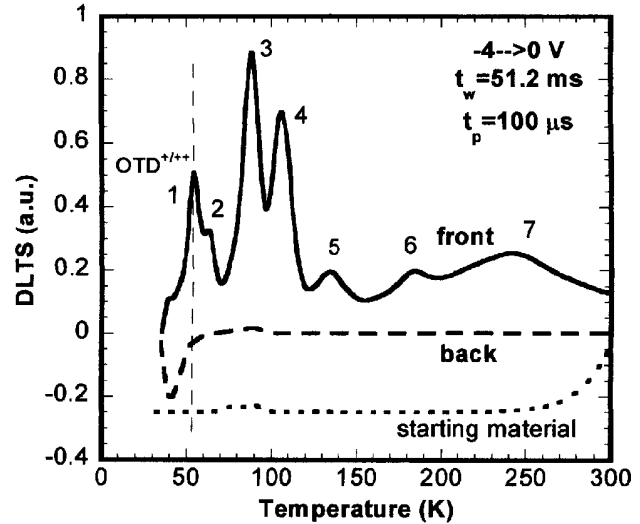


Fig. 4. DLTS spectra of specimen 3-1 in the initial state (*starting material*) and after the thermoradiation treatment at 450 °C (*front* is irradiated and *back* is unirradiated side of specimen).  $n\text{-Cz: [O]} = 2 \cdot 10^{17} \text{ cm}^{-3}$

on the specimen back sides due to the RD long-range migration.

As is seen from Table 1, for specimen 11-1, the free electron concentrations determined from the capacitor-voltage characteristics of Schottky barriers differ on the front and back sides only by a factor of three, although the compensating RD concentrations, as is seen from Fig.1, have more than tenfold difference. This means that, on the front side, there were created at least 4 times more thermal donors than on the back one. This also confirms the stimulating radiation effect on the thermal donor generation.

In order to reveal the hole capture sites (donors in the lower half of the gap), an optical injection was used in the DLTS method. The result for the front side of specimen 11-1 is shown in Fig. 3. The charge inversion of the level near 200 K is clearly seen and probably of another one near 100 K which evidences for the existence of the hole capture sites in the investigated layer.

For a more correct determination of the high-temperature RD parameters, the “hot irradiation” experiment was repeated providing the small compensation of conductivity by RDs. With this aim in view, specimen 3-1 possessing the higher initial concentration of free electrons was irradiated by minimal dose at 450 °C during the minimal period (Table 1). Due to the low content of the oxygen impurity in this crystal,

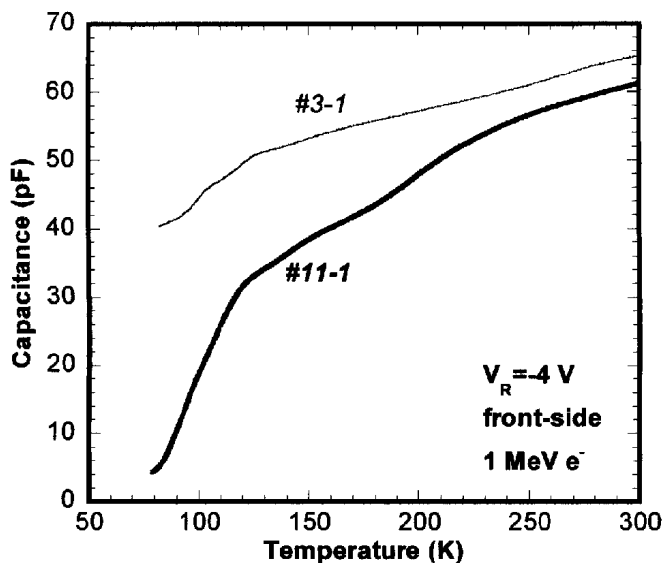


Fig. 5. Temperature dependences of the capacity of the Schottky barrier on the front sides of specimens 11-1 and 3-1. *n*-type Cz silicon

the influence of OTDs on the secondary RD generation was made minimal.

DLTS spectra were measured in a wider range of temperatures (4.2–300 K) than that in previous experiments (78–300 K). This allow us to observe three low-temperature peaks in addition to those described above. The DLTS spectrum for the side of specimen 3-1 irradiated at 450 °C is shown in Fig. 4. For comparison, the initial crystal spectrum (without radiation or thermal treatment) is also shown. All spectra are recorded under identical experimental conditions. It is seen that peak N 1 in the irradiated specimen coincides according to the temperature position with the thermal donor peak in “oxygen” crystals [11]. At the same time, on the back side of specimen 3-1, this probably “thermal-donor-induced” peak is not observed at all, as it should be for the crystal with such a low oxygen content after such a short thermal treatment [12].

For peak N 1, in contrast to the others, a dependence of the temperature position of the peak maximum on the firing pulse amplitude is observed. This dependence is described satisfactory by the theory of the Pool–Frenkel effect for a double donor. The facts quoted above make possible to identify peak N 1 as the deepest level of the double OTD. So, the large amplitude of peak N 1 on the front side of specimen 3-1, being absent on the back one, is a direct proof of the OTD generation enhancement

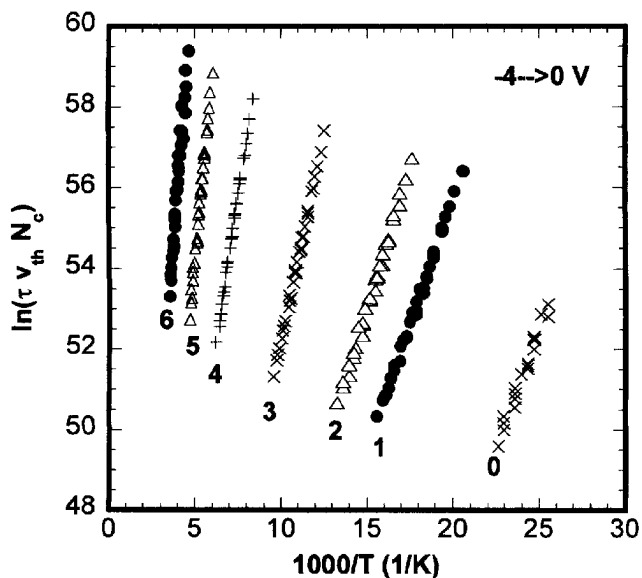


Fig. 6. Arrhenius dependences for the front side of specimen 3-1. 1 MeV electron irradiation at 450 °C

under irradiation even in Si with low content of the oxygen impurity.

Concerning peaks at higher temperatures, when comparing the spectra in Figs. 1 and 4, one may say the following. As a result of the usage of a more prolonged interval between filling pulses, the temperature arrangement of the peak maxima has changed to some extent, but their number is preserved in both materials. The peak amplitude ratio is affected essentially. In comparison with specimen 11-1, this ratio for specimen 3-1 has changed in favor of the lower-temperature peaks. Among the possible explanations can be that the compensation degree by RDs is much greater in the first experiment. Therefore, in specimen 11-1, there are not enough free electrons to fill completely shallower levels which are situated at lower temperatures in the DLTS spectra. In favor of this viewpoint serves the comparison of the temperature dependences of the barrier capacity on the front sides of specimens 11-1 and 3-1 (see Fig. 5). It is seen that, due to the freezing-up of free electrons onto the deep levels of the compensating RDs, the capacity in specimen 11-1 has the tenfold change, while only by 20–30% in specimen 3-1. This gives reasons to consider as correct the application of the Arrhenius method for the determination of the activation energy for the charge inversion of the levels which are responsible for the DLTS peaks in Fig. 4. In

Fig. 6, the Arrhenius dependences are shown for the DLTS peaks of specimen 3-1 treated thermoradiationally at 450 °C. The obtained values for parameters are quoted in Table 2. Here, the charge inversion energy  $E_T$ , the electron capture cross-section  $\sigma_n$ , and the concentration of the relevant levels  $N_T$  are listed for each peak.

Basing on those and earlier reported data, the following interpretations are possible for the origin of defects which give rise to the relevant levels in the forbidden gap of Si.

Peak N 1, according to its energy disposition and sensitivity to an electric field, can be attributed to another, deeper OTD level. Such an interpretation of peak N 1 is somewhat contradicted by its relatively small electron capture cross-section  $(1 \div 3) \cdot 10^{-14} \text{ cm}^2$ . For OTDs, the value of the order of  $10^{-13} \text{ cm}^2$  is more typical [11]. Perhaps, the early stages of the OTD formation (the thermoradiation treatment prolongs 10 min), which are characterized by a small amount of oxygen atoms in the OTDs, are responsible for such a small cross-section just due to the small geometric sizes of the OTD precipitate.

Peak N 2 can also be classified as a thermodonor level. It has a very large capture cross-section of  $7 \cdot 10^{-11} \text{ cm}^2$ . But since it is situated on the slope of the higher peak N 1, it is rather difficult to determine accurately its temperature position and hence the parameters of the relevant level.

All other peaks correspond to the levels of the  $p$ -type which may evidence for their radiation nature. Their total concentration, according to Table 2, amounts to approximately  $8.3 \cdot 10^{13} \text{ cm}^{-3}$ , and the concentration of double OTDs to  $2.3 \cdot 10^{13} \text{ cm}^{-3}$ . At the same time, the reduction of the free electron concentration after the thermoradiation treatment equals  $11 \cdot 10^{13} \text{ cm}^{-3}$ . This confirms the conclusion made above about the availability of acceptor levels in the lower half of the gap.

Peak N 3, being maximal according to the concentration, corresponds to the  $A$ -center characteristics (a VO complex) according to the charge inversion energy

and electron capture cross-section. Although the annealing temperature of the  $A$ -center is about 300–350 °C, its existence at 450 °C is possible due to the large intensity of the irradiation and the migrational nature of the annealing. The most probable drain mechanism for the vacancies created by irradiation is evidently an encounter with the oxygen impurity atoms. In this case, the appearing complexes VO (peak N 3) are annealed migrating as a whole to the drain sites, the most probable of which are also the oxygen atoms. In the course of the reaction



the  $\text{VO}_2$  complex is created, being the next in the concentration after the  $A$ -center on the initial stages of the irradiation. Peak N 4 corresponds to it. During the irradiation, those complexes are accumulated only, because the radiation dose in our experiments is of the order of  $10^{16} \text{ cm}^{-2}$  and the reactions



and



are minor. On the contrary, the amplitude of peak N 3 characterizes the equilibrium concentration of the  $A$ -centers in the double reaction



and hence does not change during the irradiation if the intensity of the latter remains constant. The cooling period of the specimen from 450 to 300 °C, after the electron beam having been switched off, is no more than 40 s. Therefore, the VO-complex concentration in reaction (4) has no time to change essentially, and its value estimated from Fig. 4 is close to the equilibrium one during the irradiation. In favor of this point of view evidences the change of the amplitude ratio for peaks Nos. 3 and 4 during the irradiation period. As is seen from Fig. 4, after the short-term irradiation (10 min), peak N 3 exceeds peak N 4 by amplitude, while the amplitude ratio changes to opposite after the long-term treatment (120 min, see Fig. 1). It is characteristic that peaks Nos. 5, 6 and 7, relatively to the  $A$ -center, also increase. It may be if those peaks correspond to more involved complexes, which are accumulated and in the generation of which the  $A$ -center takes part. This does not contradict the data of works [3, 7], where, in Si irradiated at 400 °C, there were revealed levels close by energy position. In particular, the level  $E_c - 0.36 \text{ eV}$  was attributed to the  $V_2\text{O}_2$  complex, while the levels

**Table 2**

| Peak number | $E_T$ , eV | $\sigma_n$ , $\text{cm}^2$ | $N_T$ , $\text{cm}^{-3}$ |
|-------------|------------|----------------------------|--------------------------|
| 1           | 0.106      | $2.96 \cdot 10^{-14}$      | $2.36 \cdot 10^{13}$     |
| 2           | 0.100      | $7.07 \cdot 10^{-11}$      | $6.94 \cdot 10^{12}$     |
| 3           | 0.172      | $9.64 \cdot 10^{-15}$      | $3.57 \cdot 10^{13}$     |
| 4           | 0.186      | $7 \cdot 10^{-16}$         | $2.7 \cdot 10^{13}$      |
| 5           | 0.239      | $6.37 \cdot 10^{-16}$      | $6.88 \cdot 10^{12}$     |
| 6           | 0.381      | $1.04 \cdot 10^{-14}$      | $6.08 \cdot 10^{12}$     |
| 7           | 0.463      | $9.89 \cdot 10^{-16}$      | $7.46 \cdot 10^{12}$     |

$E_c - 0.22$  eV and  $E_c - 0.47$  eV to the vacancy complexes of higher orders. One cannot exclude that some of the deep levels revealed by us are created by the complexes  $VO_2$  or  $VO_3$  which were observed in [13, 14] during the high-temperature irradiation of Si using the IR spectroscopy methods.

Thus, the results obtained allow us to make the following conclusions:

(i) Electron irradiation can essentially enhance the generation of oxygen thermal donors in Si. Taking into account that the creation of thermal donors is governed by the diffusion of oxygen impurity atoms, this result proves that the oxygen diffusion in Si is stimulated by the irradiation.

(ii) Oxygen-vacancy complexes at  $450^\circ\text{C}$  are capable to migrate in Si over the distances which greatly exceed the migration length of a free vacancy. The transportation of the oxygen atoms in the content of such complexes can be one of the mechanisms of the radiation-enhanced diffusion.

(iii) The  $A$ -center remains the dominant secondary radiation-induced defect in the early stages of the irradiation at the temperature  $450^\circ\text{C}$  as well. This evidences for that its annealing occurs by means of the migration to the drain sites rather than the dissociation. Therefore, the  $A$ -center represents the intermediate stage in the process of creation of more involved complexes of the type  $V_xO_y$ .

1. *Claeys C., Simoen E.* Radiation Effects in Advanced Semiconductor Materials and Devices. — Springer Series in Materials Science, 2002. — Pt. 3.
2. *Lévêque P., Nielsen H.K., Pellegrino P. et al.*// J. Appl. Phys. **93** (2003) 871.
3. *Xu J.-G., Lu F., Sun H.-H.*// Phys. Rev. B. **38** (1988) 3395.
4. *Emtsev V.V., Daluda Yu.N., Shakhovtsov V.I. et al.*// Fiz. Tekhn. Polupr. **24** (1990) 374–377.
5. *Hazdra P., Haslar V., Bartos VM.*// Nucl. Instrum. Methods in Phys. Res. B. **55** (1991) 637.

6. *Lalita J., Svensson B.G., Jagdish C.*// Ibid. **96** (1995) 210.
7. *Schmidt D.C., Svensson B.G., Lindström J.L. et al.*// J. Appl. Phys. **85** (1999) 3556.
8. *Oates A.S., Binns M.J., Newman R.C. et al.*// J. Phys. C: Solid State Phys. **17** (1984) 5695.
9. *Neimash V.B., Kras'ko M.M., Kraitchinskii A.M.*// Ukr. Fiz. Zh. **47** (2002) 50.
10. *Neimash V., Kraitchinskii A., Kras'ko M. et al.*// Proc. High Purity Silicon VII/ Eds. C. Claeys, P. Rai-Choudhury, M. Watanabe, P. Stallhofer. — The Electrochem. Soc. Ser. PV 2002-20. — 2002. — P. 278–289.
11. *Benton J.L., Kimerling L.C., Stavola M.*// Physica B. **116** (1983) 271.
12. *Babich V.M., Bletska N.I., Venger E.F.* Oxygen in Silicon Single Crystals. — Kyiv: Interpress LTD, 1997 (in Russian).
13. *Lindström J.L., Hallberg T., Aberg D. et al.*// Mat. Sci. Forum. **258-263** (1997) 367.
14. *Lindström J.L., Murin L.I., Hallberg T. et al.*// Nucl. Instrum. Meth. in Phys. Res. B. **186** (2002) 121.

Received 08.07.03.

Translated from Ukrainian by O.I. Voitenko

#### ДОСЛІДЖЕННЯ ЄМНІСНИМИ МЕТОДАМИ $n$ -КРЕМНІЮ, ОПРОМІНЕНОГО ЕЛЕКТРОНАМИ ПРИ $450^\circ\text{C}$

*В.Б. Неймаш, М.М. Красько, А.М. Крайчинський, А.Г. Колосюк, В.В. Войтович, Е.Сімоєн, Дж.-М. Рафі, К.Клайз, Дж.Верслауз, П.Клоз*

#### Резюме

Методами ємнісної спектроскопії глибоких рівнів досліджено властивості радіаційних та термічних дефектів, що утворюються в монокристалічному Si при 1 MeV електронному опроміненні при  $450^\circ\text{C}$ . Виявлено сім електронних рівнів у верхній та два рівня у нижній половині забороненої зони Si. Визначено їх енергетичні та кінетичні характеристики. Встановлено, що вторинні радіаційні дефекти здатні до міграції на великі відстані. Показано значне прискорення генерації кисневих термодонорів під дією електронного опромінення. Отримані результати інтерпретовано радіаційно прискореною дифузиею атомів домішки кисню та формуванням різних кисневмісних комплексів.